31st Congress of the International Council of the Aeronautical Sciences

Belo Horizonte, Brazil; September 09-14, 2018

ON THE WAVE-CANCELLING NATURE OF BOUNDARY LAYER TRANSITION CONTROL

Kenzo Sasaki* , **Pierluigi Morra**** , **André V. G. Cavalieri*** , **Ardeshir Hanifi**** , **Dan S. Henningson****

***Instituto Tecnológico de Aeronáutica, São José dos Campos, SP, 12228-900, Brazil ,**

****KTH Royal Institute of Technology, Stockholm, SE-100-44, Sweden**

Keywords: *Flow control, Tollmien-Schlichting waves, feedforward control.*

Abstract

This work deals with the feedforward active control of velocity fluctuations over incompressible 3D boundary layers. Two strategies are evaluated, the Linear Quadratic Gaussian (LQG) controller, built using the eigensystem realization algorithm (ERA), is compared to a wave-cancellation scheme, obtained via the direct inversion of the frequency-domain transfer functions of the system. For the evaluated cases, it is shown that LQG leads to a wave-cancelling signal of the incoming Tollmien-Schlichting wavepacket. Such result allows further insight into the physics behind the active control of convectively unstable flows permitting, for instance, the optimization of the transverse position for actuation via a linear stability approach.

1 General Introduction

The manipulation of the flow dynamics via passive or active control strategies poses a challenge with several foreseeable industrial and technological applications, and there is a particular interest in the delay of the laminar-turbulent transition of a boundary layer and consequent drag reduction, as the main expenses of a commercial airline are related to fuel consumptions [1].

In a low free-stream turbulence environment, transition of unswept wings is most often due to Tollmien-Schlichting (TS) waves which, depending on the Reynolds number of the flow, will grow exponentially until a critical amplitude will lead to non-linear interactions [2] and finally breakdown to turbulence. In general, the actuation is placed in a region where the amplitude of the TS waves is small, and the convective nature of the flow is accounted via a feedforward scheme, where the input signal is not affected by the actuation. Several examples of this type of control may be found in the literature; for instance Fabbiane *et al.* [4, 3] apply linear-quadratic-Gaussian (LQG) and adaptive schemes and Li & Gaster [5] consider an inversion of transfer functions for the active control of 3D boundary-layers.

The work of Fabbiane *et al.* [3] evaluates the energy budget related to active control and demonstrates that, even though the actuation is performed in a region of low amplitude of the TS waves, with the currently available flow control actuators, it can difficult to obtain drag reductions below the energy break-even point, for their evaluated cases.

With this in mind, we propose an inversion technique based on the nature of the convectively unstable flow and show that the more complex LQG controller reduces to such strategy, in the frequencies of interest for control, leading to a wave-cancellation scheme. The control law is similar to the one proposed in Li & Gaster [5], however a penalization of the actuation signal is also included, which allows uncontrollable frequencies to be disregarded and increases the

robustness of the system with respect to noise and model uncertainties. Knowledge that the closed-loop control acts via a wave-cancelling signal allows a further stability analysis to improve the shape of actuation in order to diminish the amplitude of actuation.

2 Methods and Baseline case for study

The incompressible Navier-Stokes equations model the flow,

$$\frac{\partial \mathbf{u}}{\partial t} + (\mathbf{u}\cdot\nabla)\mathbf{u} = -\nabla p + \frac{1}{Re}\nabla^2\mathbf{u} + \lambda(x)\mathbf{u} + \mathbf{f} \quad (1)$$

$$\nabla\cdot\mathbf{u} = 0 \quad (2)$$

where $\mathbf{u}(\mathbf{x},t)$ and $p(\mathbf{x},t)$ are the velocity and pressure, respectively, at each time step t and position $\mathbf{x} = (X_1, X_2, X_3)$, taken in the cartesian coordinates. The streamwise direction X_1 is aligned with the free-stream velocity U_∞, X_2 is normal to the surface of the plate and X_3 defines a spanwise direction. Two-dimensional and three-dimensional simulations are performed; for the former, the dependence of the quantities along the spanwise direction is not considered.
A plate of semi-infinite length lies in the X_1X_3 plane, where no-slip conditions are enforced at $X_2 = 0$. Direct Numerical Simulations (DNS) using the spectral code SIMSON are performed to analyse the control action. The flow is periodic along the spanwise direction and a fringe forcing, given as $\lambda(x)$, introduced in the last 20% of the domain, ensures periodicity also along the streamwise direction [7]. These periodic directions are discretised using a Fourier basis, and for the wall-normal direction Chebyshev polynomials are used. Figure 2 presents a scheme of the simulation and coordinates considered.

Spatial coordinates and velocities are non-dimensionalized using the displacement thickness δ^* in the entrance of the domain and the free-stream velocity U_∞, respectively. The resulting Reynolds number, defined as $Re = \delta^* U_\infty/\nu$,

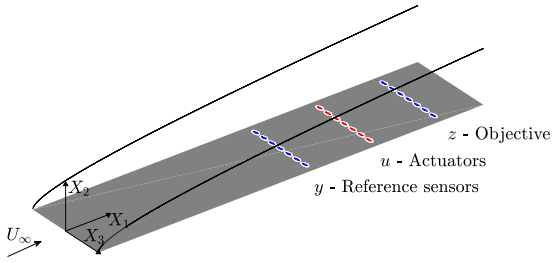

Fig. 1 Scheme for the 3D simulation of the flat plate considered. The blue and red circles represent the input sensors and actuators, respectively.

where ν is the kinematic viscosity, is 1000. Time integration is performed using the fourth-order Crank-Nicholson/Runge-Kutta method, with a constant non-dimensional time step of $\Delta t = 0.4$. The computational domain for the 3D simulation is of $[0,1000]\times[0,30]\times[-70,70]$ in the X_1, X_2 and X_3 directions, with $N_{x_1} = 768$ and $N_{x_3} = 96$ Fourier modes at the X_1X_3 plane and $N_{x_2} = 101$ Chebyshev polynomials at the vertical direction. The 2D simulation is performed with the same X_1X_2 configurations.
A volume forcing f is used both to introduce random disturbances and to perform the control action. The forcing is divergent-free, consisting of localized synthetic vortices [6], with spatial support given as

$$\mathbf{b} = \left[\chi\tilde{X_2}, -\gamma\tilde{X_1}, 0\right]\exp(-\tilde{X_1}^2 - \tilde{X_2}^2 - \tilde{X_3}^2) \quad (3)$$

where $\tilde{X_1} = (X_1 - X_{10})/\chi$, $\tilde{X_2} = (X_2 - X_{20})/\gamma$ and $\tilde{X_3} = (X_3 - X_{30})/\zeta$, such that X_{10}, X_{20} and X_{30} indicate the position where the disturbance is centred and χ, γ and ζ the spatial decay of the force. A random broadband signal $d(t)$ modulates the forcing at the position of upstream perturbations, whereas a control signal $u(t)$ determines the actuation signal at the position X_{1u}.
A localized measurement of the streamwise skin friction is used to define the inputs given by sensors $y(t)$, and downstream objective, $z(t)$. Four rows of equispaced independent objects are placed with a transverse separation of $\Delta X_3 = 10$

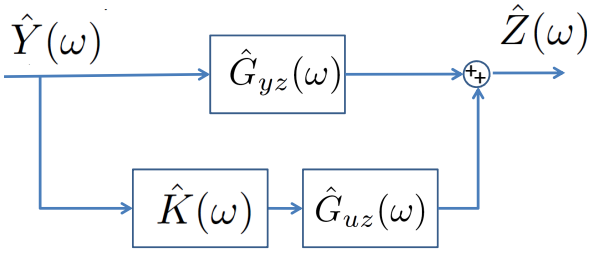

Fig. 2 Resulting block diagram for feedforward control.

for the 3D simulation. Disturbances are added at the wall, at $X_{1d} = 35$, measurements are taken at $X_{1y} = 300$ and $X_{1z} = 500$, defining input and objective, respectively. Actuation is performed at $X_{1u} = 400$, both on the wall, for the baseline case, and at an optimized position to be discussed later.

The scheme we consider for control is reactive to input behaviour, with input upstream of the actuation, leading to a feedforward scheme, as the flow is strongly convective. Figure 2 presents the resulting block diagram for this purpose, the transfer function $\hat{G}_{yz}(\omega)$, where ω is the angular frequency, determines the relation between input position and objective, y, u and z are input, actuation and output respectively.
Such transfer functions were obtained from three strategies: the Fourier transform of the impulse responses of the system, an empirical frequency-response or using theoretically constructed by means of solutions of the parabolized stability equations (PSE) [12].

The role of the controller will be to determine the kernel such that the actuation, described via a finite impulse response filter (FIR), which reads

$$u(t) = \int_0^{+\infty} k(\tau) y(t-\tau) d\tau \qquad (4)$$

The kernel $k(t)$ defines the control law, and two cases will be considered. The first is optimal linear quadratic gaussian [9] applied to a reduced-order model of the linearized system obtained with the eigensystem realization algorithm[10]; the second is the direct inversion of the system, performed in the frequency-domain from the impulse responses of the linearized simulation. For the latter, we superpose the open-loop signal with an actuation, such that the Fourier-transformed output is given by

$$\hat{Z}(\omega) = \hat{Y}(\omega)\hat{G}_{yz}(\omega) + \hat{U}(\omega)\hat{G}_{uz}(\omega) \qquad (5)$$

and minimize the functional,

$$J = \int_{-\infty}^{\infty} \left[\hat{U}^*(\omega)R(\omega)\hat{U}(\omega) + \hat{Z}(\omega)^* Q(\omega)\hat{Z}\right] d\omega \qquad (6)$$

defined in the frequency-domain, which penalizes both actuation and output. We take $\hat{U}(\omega) = \hat{K}(\omega)\hat{Y}(\omega)$, and the inverse Fourier transform of $\hat{K}(\omega)$ will lead to a FIR format such that the actuation is computed via equation 4. This procedure, which we will refer to as wave-cancellation, has the added advantage of not depending on the step of building a reduced-order model for computation of the control, dealing directly with the transfer functions obtained using impulse responses of the system.
The extension of this method and the resulting kernels for a 3D boundary layer involves a second Fourier transform, from X_3 to the transverse wavenumber β, and this derivation may be found in Sasaki *et al.* [11].
The actuation for the 3D boundary layer, written in its discretized form, for $M+1$ sensors and actuators is given by a double discrete convolution of the measurements with the kernel, using a buffer of N points for the the time discretization:

$$u_l(n) = \sum_{m=-M/2}^{M/2} \sum_{j=0}^{N} k_m(j) y_{l-m}(n-j), \qquad (7)$$

The baseline case for study considers the streamwise positions of $X_1 = 300$, 400 and 500 for input, actuation and output, respectively; inflow disturbances are inserted at $X_1 = 35$.

3 Results

Figure 3 shows the LQG and wave-cancellation kernels, which were calculated by evaluating the penalizations of the state and actuation in order to

obtain the best performance in terms of the reduction of the objective signal. The objective corresponds to the axial velocity perturbations which develop on top of the laminar, unperturbed, solution.

The resulting shear of the axial velocity is given in figure 4, with respect to its laminar unperturbed solution, for the uncontrolled and controlled cases.

There is a reduction of 75% on the mean-square value of the shear of the velocity fluctuations on the wall, for both controllers. The corresponding actuation for both of the evaluated control strategies is equivalent, with both the shape and amplitude of the kernels being similar. Although not shown here, both strategies presented adequate robustness characteristics on what concerns the amplitude of perturbations, plant uncertainties given in terms of the Reynolds number and noise in the sensors and actuators.

The results of this section indicate that the closed-loop actuation, for both of the evaluated controllers, is acting by means of a wave-cancelling signal of the incoming Tollmien-Schlichting wavepacket. This destructive interference occurs downstream of the actuation position. By acknowledging this fact, it is possible to use the PSE derived transfer functions and concepts of linear stability in order to improve the position of actuation, displacing it above of the wall, to an improved transverse location. The method to perform this analysis is outlined in detail in Sasaki *et al.* [11].

The idea concerns the use of the position of the critical layer, where the receptivity of the flow to perturbation is greatest [13], and then consider the different amplification rates of each frequency by means of the PSE transfer function. The wave-cancellation and LQG kernels were computed for the same objective position but considering the optimized transverse position of actuation $X_{2_{opt}}$. The results of this procedure are summarized in table 1, which considered simulations over the 2D boundary layer.

Table 1 indicates that by acting on the improved transverse position it is possible to

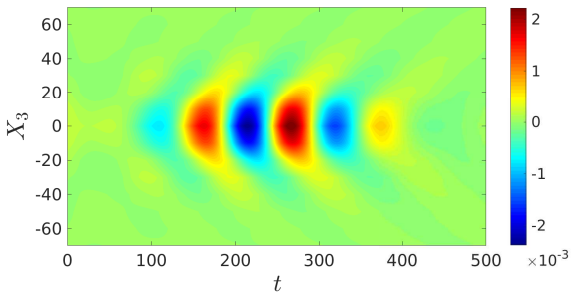

(a) LQG - Continuous

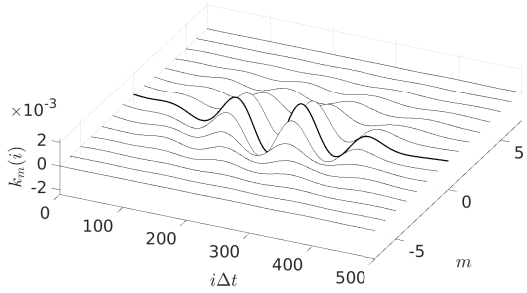

(b) LQG - Discrete

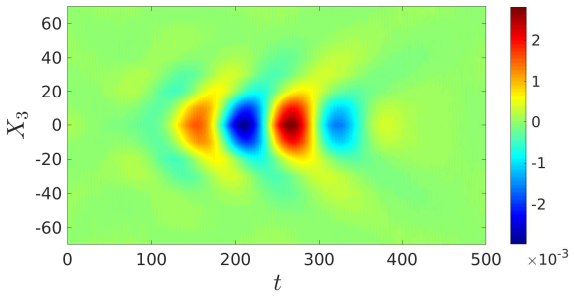

(c) Wave-cancellation - Continuous

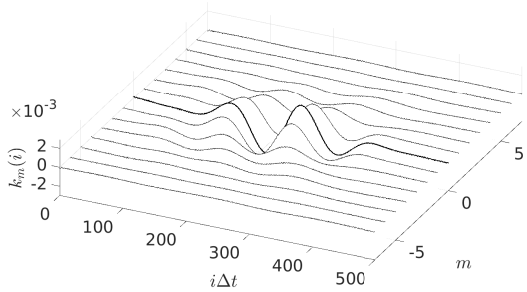

(d) Wave-cancellation - Discrete

Fig. 3 Behaviour of the LQG and wave-cancellation kernels with the respective chosen penalizations in a continuous and discretized formalism. The index m indicates the position of the actuators, with $m = 0$ indicating an aligned actuator/sensor pair.

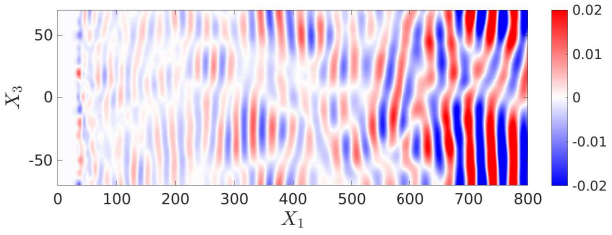

(a) Uncontrolled

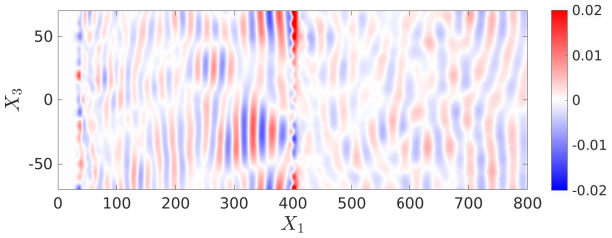

(b) Controlled - Wave Cancellation

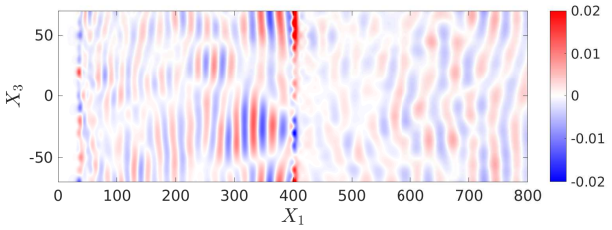

(c) Controlled - LQG

Fig. 4 Behaviour of the shear of the velocity fluctuation with respect to the laminar value, comparison between uncontrolled and controlled cases.

Controller	u^2	z^2
Uncontrolled case	-	399
LQG - Wall	0.281	0.001
LQG - $X_{2_{opt}}$	0.004	0.001
Wave-cancellation - Wall	0.281	0.002
Wave-cancellation - $X_{2_{opt}}$	0.004	0.003

Table 1 Summary of the closed-loop cases evaluated.

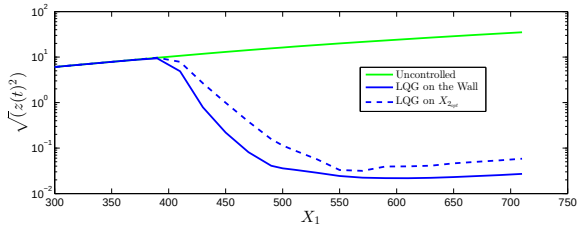

(a)

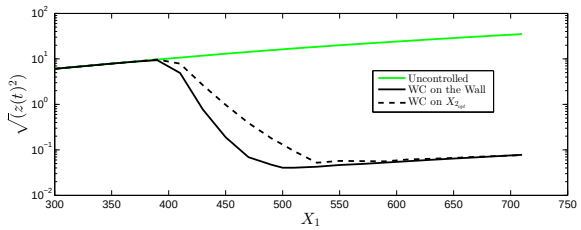

(b)

Fig. 5 Comparison of the rms values of the output, for the 2D simulation for actuation on the wall and at the optimal position. (a) LQG (b) Wave-cancellation

diminish the actuation power by two orders of magnitude without any significant loss of performance in the closed-loop behaviour.
Figure 5 presents the rms of the axial velocity fluctuation as a function of the axial position and confirms the reduction of the axial velocity remains downstream of actuation. The same behaviour is also observed for the wave cancellation control.

4 Conclusions

Two techniques were evaluated for the closed-loop control of streamwise velocity fluctuations in a transitional 3D boundary layer. The linear quadratic gaussian regulator, built using an eigensystem realization algorithm, was shown to lead to equivalent results, in terms of actuation and closed-loop performance, to the simpler wave-cancellation kernels. This trend gives insight into the physical mechanisms behind flow control and allowed the use of linear stability tools to aid on the design of an actuator which would more efficiently generate TS waves that

cancel incoming ones.
Via these ideas, an improved position for actuation was determined. This result presents a proof of concept, demonstrating that there is room for significant improvements of the current available actuators which could allow to go beyond the break even point highlighted in Fabbiane *et al.*, 2017 [3]. This may also serve as a guideline for the design of actuators for flow control, where the wave-cancellation scheme presents a fast method to perform parametric evaluations and sensor/actuator placement.

5 Acknowledgements

Part of this work has been developed during an exchange programme to KTH, when the first author appreciated a scholarship from Capes, project number 88881.132008/2016-01. Kenzo Sasaki has received a scholarship from FAPESP, grant number 2016/25187-4. André V. G. Cavalieri was supported by a CNPq grant 44796/2014-2. The authors would also like to acknowledge the funding from PreLaFloDes, Swedemo and CISB (Swedish-Brazilian Research and Innovation Centre). Simulations have been performed at National Supercomputer Centre (NSC) and High Performance Computing Center North (HPC2N) with computer time provided by the Swedish National Infrastructure for Computing (SNIC).

References

[1] Schrauf G., *Status and perspectives of laminar flow.* The aeronautical journal 109 (1102), 639-644.

[2] Kachanov, Y. S., *Physical mechanisms of laminar boundary-layer transition.* Annual review of fluid mechanics, vol. 26, no. 1, pp. 411-482, 1994.

[3] Fabbiane N., Bagheri S., Henningson D. S., *Energy efficiency and performance limitations of linear adaptive control for transition delay.* Journal of Fluid Mechanics, vol. 810, pp. 60-81, 2017

[4] Fabbiane N., Simon B., Fischer F., Grundmann S., Bagheri S., Henningson D. S., *On the role of adaptivity for robust laminar flow control.* Journal of Fluid Mechanics, vol. 767, o. R1, 2015.

[5] Li Y., Gaster M., *Active control of boundary-layer instabilities.* Journal of Fluid Mechanics, vol. 550, pp. 185-205, 2006.

[6] Semeraro O., Bagheri S., Brandt L., Henningson D. S., *Transition delay in boundary layers using active control.* Journal of Fluid Mechanics, vol. 731, pp. 288-311, 2013.

[7] Nordström J., Nordin N., Henningson D. S., *The fringe region technique and the Fourier method used in the direct numerical simulation of spatially evolving viscous flows.* SIAM Journal on Scientific Computing, vol. 20, number 4, pp. 1365-1393, 1999.

[8] Chevalier M., Lundbladh A., Henningson D. S., *Simson a pseudo-spectral solver for incompressible boundary layer flow.* Tech. Rep., TRITA-MEK, 2007.

[9] Bagheri S., Henningson D. S., Hoepffner J., Schmid P. J., *Input-output analysis and control design applied to a linear model of spatially developing flows.* Applied Mechanics Reviews, vol. 62, no 2, p. 020803, 2009.

[10] Juang J. N., Pappa R. S., *An eigensystem realization algorithm for modal parameter identification and model reduction.* Journal of Guidance 8(5), 620-627 (1985).

[11] Sasaki K., Morra P., Fabbiane N., Cavalieri A. V. G., Hanifi, A., Henningson D. S., *On the wave-cancelling nature of boundary layer flow control.* Theoretical and Computational Fluid Dynamics, *accepted for publication*.

[12] Sasaki K. Piantanida S., Cavalieri A. V. G., Jordan P. *Real-time modelling of wavepackets in turbulent jets.* Journal of Fluid Mechanics, vol. 821, pp. 458-481.

[13] Hill D. C. *Adjoint systems and their role in the receptivity problem for boundary layers.* Journal of Fluid Mechanics, vol. 292, pp. 183-204, 1995.

6 Contact Author Email Address

Email: kenzo@ita.br

Copyright Statement

The authors confirm that they, and/or their company or organization, hold copyright on all of the original material included in this paper. The authors also confirm that they have obtained permission, from the copyright holder of any third party material included in this paper, to publish it as part of their paper. The authors confirm that they give permission, or have obtained permission from the copyright holder of this paper, for the publication and distribution of this paper as part of the ICAS proceedings or as individual off-prints from the proceedings.